

**Negative and positive hysteresis in double-cavity optical bistability in a three-level atom**

H. Aswath Babu and Harshawardhan Wanare\*

*Department of Physics, Indian Institute of Technology, Kanpur 208 016, India*

(Received 8 September 2010; published 18 March 2011; publisher error corrected 24 March 2011)

We present dual hysteretic behavior of a three-level ladder system exhibiting optical bistability in a double-cavity configuration in the mean-field limit. The two fields coupling the atomic system experience competing cooperative effects along the two transitions. We observe a hump-like feature in the bistable curve arising due to cavity-induced inversion, which transforms into a negative-hysteresis loop. Apart from negative- and positive-hysteresis regions, the system offers a variety of controllable nonlinear dynamical features, ranging from switching, periodic self-pulsing to chaos.

DOI: [10.1103/PhysRevA.83.033818](https://doi.org/10.1103/PhysRevA.83.033818)

PACS number(s): 42.65.Pc, 42.50.Gy, 42.65.Sf

**I. INTRODUCTION**

All-optical bistability has been the focus of research for more than four decades [1,2], apart from its potential application as a switch [3] in optical communication technology; it remains a test bed for fundamental research. Issues related to cooperative phenomena [4] as well as the study of nonlinear dynamical aspects, such as self-pulsing, instabilities, and chaos, have been extensively undertaken [5]. A deeper understanding of issues related to quantum aspects such as entanglement and cooperative behavior in the presence or absence of instabilities would be critical in realizing a functional quantum computer. Due to recent developments related to cold atoms in optical lattices [6] and atomic chips [7], the aspects related to cooperative phenomena have become vital [8]. Design of a smaller trap ( $<\lambda$ ) demands a treatment that allows for cooperative effects, and possibly at multiple frequencies, which can be realized in multilevel atoms. We show the onset of instabilities in such systems at low input light levels. Multilevel atoms have been used recently to create and control cooperative effects, such as in multiparticle dark states [9] and Rydberg blockade effects [10] in cold atoms in a trap. To understand the interplay of multicolored cooperative effects, we explore the semiclassical dynamics of two fields coupling two adjacent transitions at which they exhibit cooperative behavior simultaneously. The atomic level structure itself provides the coupling between the two distinct cooperative branches.

In an early work, one of the authors (H.W., with G.S. Agarwal) showed the possibility of control of optical bistability (OB) [11] in a three-level atomic medium, where the OB exhibited by one (probe) field is controlled by another (control) field coupling an adjacent transition. The field exhibiting bistability experiences conventional cavity feedback, whereas the control field is held constant without feedback. The necessary condition for the field to exhibit cooperative behavior arises from a strong interaction with the active media accompanied by sufficient feedback. An external cavity configuration allows effective engineering of various characteristics of OB, including tailoring of thresholds, changing the on and off intensities of the output field, and obtaining multistability [12]. These effects were also

experimentally realized [13]. Furthermore, the three-level atom with a control field (without feedback) has been shown to exhibit instability in the context of OB [14].

In this work, we have two fields that couple to two adjacent transitions in a three-level atom, however, both the fields experience feedback via two independent, single-mode, unidirectional ring cavities, as indicated in Fig. 1. This system provides independent control over the two cooperative parameters via the transmission coefficient of the cavity. This configuration leads to *negative* hysteresis apart from the conventional positive bistable hysteresis. The fields are chosen to be counter-propagating within the active medium in order to minimize the two-photon Doppler broadening [15], however, our calculation is undertaken for a homogeneously broadened atomic gas. Conjoined hysteresis (positive and negative) has been observed experimentally and may require a theoretical model involving six-wave mixing within a three-level  $\lambda$  system [16].

Nonlinear dynamics related to OB has traditionally been associated with the inclusion of multimodal treatment of the cavity field [2,17], here, we have just two single modes corresponding to the two monochromatic fields coupling the atom. The theory of two-photon amplifiers and absorbers forms the traditional basis of studying these systems, which traditionally reduces the problem to an effective two-level model and has been extensively studied [18]. Along similar lines, two-photon, double-beam OB has been modeled [19], however, such an analysis disregards the decay channels associated with the intermediate state. Our model explicitly incorporates these effects by considering the single-photon coupling to the intermediate state. Previously chaos has also been obtained for atoms interacting with a single mode, where chaos occurs in the upper branch for extremely large cooperative parameters accompanied by large atomic and cavity detunings [20]. There have been other studies relating to the dispersive regime of two-photon OB, which deals with the effects of cavity detuning that controls both the fields simultaneously [21]. Here, the system exhibits chaos at sufficiently low input light levels in the lower branch of the OB response without being restricted to any special dispersive regime. The rich nonlinear dynamical features arise due to the *interplay* of the two cooperative phenomena.

Apart from nonlinear dynamics, the system exhibits cavity-induced inversion and positive as well as negative hysteresis

\*hwanare@iitk.ac.in

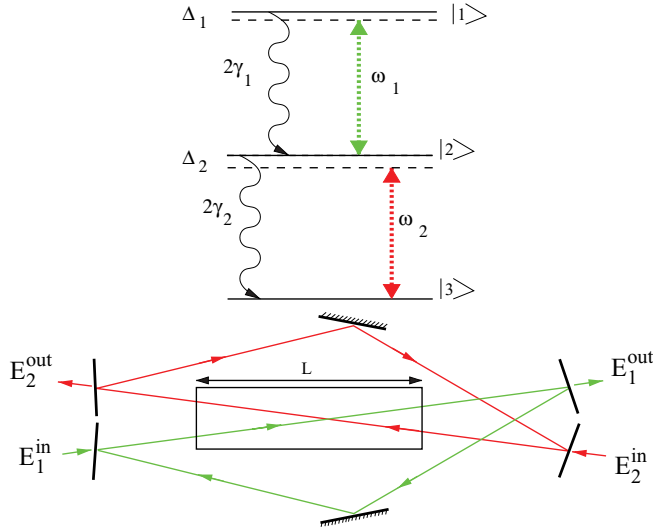


FIG. 1. (Color online) Top: Schematic of the three-level ladder system interacting with the two fields  $E_1$  and  $E_2$  at frequencies  $\omega_1$  and  $\omega_2$ , respectively. Bottom: OB setup with the collection of atoms (within the length  $L$ ) that interact with the two fields in two independent ring cavities.

in distinct input intensity regimes. Our results are in contradiction to those reported earlier; in particular, we observe an enhanced output field resulting from the creation of population inversion between state  $|1\rangle$  and state  $|2\rangle$ , in the presence of concurrent feedback for fields coupling *both* transitions. The effects are particularly significant, as they occur at the onset of the lower branch and could be used as a nonlinear component in optical circuitry. Details of the nonlinear dynamical studies are presented in the companion paper [22].

## II. MODEL SYSTEM

The atom-field density matrix equations and the field equations in terms of scaled output field ( $x_1 = d_{12}E_1^{\text{out}}/\hbar\gamma_1\sqrt{T_1}$ ,  $x_2 = d_{23}E_2^{\text{out}}/\hbar\gamma_2\sqrt{T_2}$ ) and input field ( $y_i$  obtained by replacing  $E_i^{\text{out}}$  by  $E_i^{\text{in}}$  in  $x_i$  for  $i = 1, 2$ ) variables governing the dynamics of the OB system in the mean-field limit are given as

$$\begin{aligned} \frac{\partial \rho}{\partial t} &= -\frac{i}{\hbar}[\hat{H}, \rho] + \hat{\mathcal{L}}\rho, \\ \frac{\partial x_1}{\partial t} &= \kappa_1 [-x_1(1 + i\theta_1) + y_1 + 2iC_1\rho_{12}], \\ \frac{\partial x_2}{\partial t} &= \kappa_2 [-x_2(1 + i\theta_2) + y_2 + 2iC_2\rho_{23}]. \end{aligned} \quad (1)$$

These equations describe the three-level atom coupled to the two fields at frequencies  $\omega_1$  and  $\omega_2$ , which experience feedback through two independent cavities characterized by cavity decay  $\kappa_1$  and  $\kappa_2$ , with cavity detuning  $\delta_1$  and  $\delta_2$  (scaled as  $\theta_i = \delta_i/T_i$ ), and cooperative parameters  $C_1$  and  $C_2$  ( $C_i = \alpha_i L/2T_i$ , where  $\alpha_i$  is the absorption coefficient, and  $T_i$  is the transmission coefficient for the field at  $\omega_i$ ), respectively. The total Hamiltonian in the dipole approximation after performing the rotating wave approximation is given as  $\hat{H} = \hbar(\Delta_1 + \Delta_2)|1\rangle\langle 1| + \hbar\Delta_2|2\rangle\langle 2| - (d_{12}E_1|1\rangle\langle 2| + d_{23}E_2|2\rangle\langle 3| + \text{H.c.})$ , where  $\Delta_1$  and  $\Delta_2$  are

the atomic detunings. Relaxation processes like spontaneous emission and dephasing of the atomic coherence are contained in the Liouville operator  $\hat{\mathcal{L}}$ . The detailed density matrix equations and the scaling of field variables along the lines of Ref. [2] are all explicitly given in Ref. [22].

We consider the mean-field limit wherein a single pass through the ring cavity only marginally affects the fields, and the strong cooperative nature arises due to the extremely long photon lifetime of the fields within the cavity, as the transmission coefficient of the cavity mirrors is chosen to be negligibly small. Under steady-state conditions one can obtain the bistable behavior for different combinations of the input and output fields. We first describe the analytical results pertaining to the absorptive double-beam OB. In the context of the general solution associated with the three-level system, we obtain nonlinear dynamics and we discuss the various domains of stability for different input field strengths through a stability domain map presented in Ref. [22], wherein regions of stable switching and unstable regions that exhibit self-pulsing and chaotic dynamics are clearly identified. The switching threshold, and the range of input fields exhibiting bistability are all dependent on parameters such as the decay rates (both atomic and for the cavity), detunings (both atomic and for the cavity), and cooperative parameters corresponding to the two transitions.

## III. RESULTS AND DISCUSSION

We begin with the description of absorptive double-cavity OB, wherein both fields are chosen to be on resonance (i.e.,  $\Delta_i = \theta_i = 0$ ) and thus can be considered real without loss of generality. For the atomic decay  $\gamma_i = 1$ , Eqs. (1) can be solved in the steady state to obtain

$$y_1 = x_1 \left[ 1 + \frac{4C_1 x_2^2}{(2 + x_1^2 + x_2^2)(1 + x_1^2 + 2x_2^2)} \right], \quad (2)$$

$$y_2 = x_2 \left[ 1 + \frac{2C_2}{(1 + x_1^2 + 2x_2^2)} \right]. \quad (3)$$

It is clear that in the absence of the  $\omega_1$  field (i.e.,  $x_1 = 0$ ), Eq. (3) reduces to the well-known Bonifacio-Lugiato OB equation

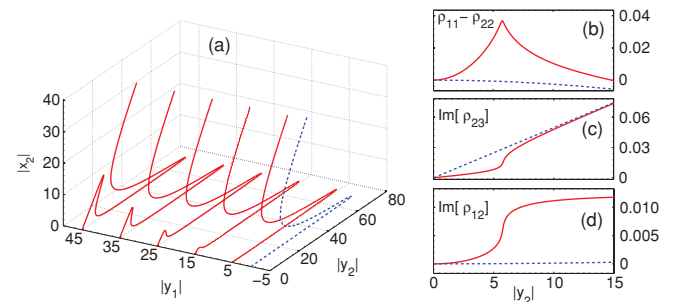


FIG. 2. (Color online) (a) Bistable response of the field at  $\omega_2$  for  $\omega_1$  fields of various strengths. Solid (red) curves indicate (b) the population inversion on the  $|1\rangle \leftrightarrow |2\rangle$  transition, (c)  $\text{Im}\{\rho_{23}\}$ , and (d)  $\text{Im}\{\rho_{12}\}$  for  $|y_1| = 25$ . Dashed (blue) lines indicate the response without feedback for the  $\omega_1$  field ( $C_1 = 0$ ,  $|y_1| = 0.05$ ). Other relevant parameters are  $C_1 = 1000$ ,  $C_2 = 100$ ,  $\kappa_i = 1$ ,  $\gamma_i = 1$ ,  $\Delta_i = 0$ , and  $\theta_i = 0$  for  $i = 1, 2$ .

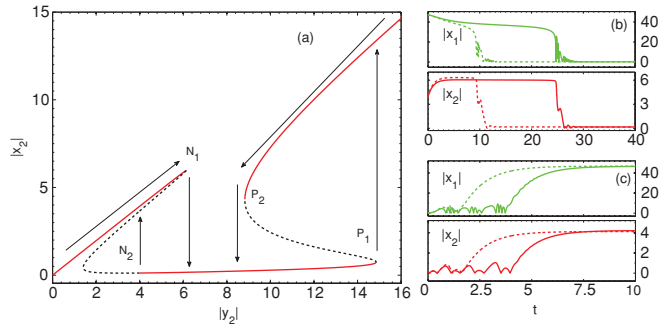


FIG. 3. (Color online) (a) Negative and positive hysteresis exhibited by the  $\omega_2$  field (for  $C_1 = 5000$ ,  $C_2 = 20$ ,  $|y_1| = 50$ ); arrows indicate the associated switching. Solid (red) and dashed (black) curves indicate stable and unstable steady-state responses, respectively. (b, c) The critical slowing-down of the negative-hysteresis loop along  $N_1$  and  $N_2$  switching, respectively. Dashed (solid) lines indicate operating points far from (closer to) the threshold. For switching at  $N_1$ ,  $|y_2|_{\text{th}} = 6.13$ ,  $|y_2|_{\text{op}} = 6.5$  (dashed),  $|y_2|_{\text{op}} = 6.2$  (solid); for switching at  $N_2$ ,  $|y_2|_{\text{th}} = 4.05$ ,  $|y_2|_{\text{op}} = 3.5$  (dashed),  $|y_2|_{\text{op}} = 3.6$  (solid). Time  $t$  is in the units of  $\kappa_1^{-1}$  and other relevant parameters are the same as in the caption to Fig. 2.

for the two-level atom [23]. To solve Eqs. (2) and (3) self-consistently, we fix the input field  $y_1$  of the upper transition and obtain the cavity field  $x_2^2$  as a function of the  $x_1$  field. The two solutions of  $x_2^2$  obtained from Eq. (2) are responsible for the negative- as well as the positive-hysteresis branches of the ( $x_2$  versus  $y_2$ ) OB response. These solutions of  $x_2^2$  can be further substituted in (3) to obtain  $y_2$  as  $x_1$  is varied, resulting in the solutions plotted in Figs. 2(a) and 3(a). It is clear from Eq. (3) that the new bistable roots appear in the lower branch (prior to the positive bistable threshold), as Eq. (3) involves a positive definite contribution from the  $x_1^2$  term in the denominator. In the general dispersive case, the above methodology fails, as these equations involve sixth and seventh powers of the fields  $x_1$  and  $x_2$ , apart from the fields themselves becoming complex, and their relative phases play a crucial role in obtaining the dynamics.

In the context of nonlinear dynamics the corresponding phase space, as well as the parameter space, is exceedingly large, owing to 12 physical parameters ( $\gamma_{1,2}$ ,  $\Delta_{1,2}$ ,  $\theta_{1,2}$ ,  $\kappa_{1,2}$ ,  $C_{1,2}$ , and  $E_{1,2}^{\text{in}}$ ) all of which can be chosen independently. With regard to the numerical implementation we express a note of caution, as this system does not permit an *a priori* choice of both the (complex) output fields. In the conventional computation of OB involving feedback for one field, one usually specifies the output field (which can be chosen to be a real value) and calculate the requisite unique (complex) input field. Such a strategy is conventionally adopted due to the multivalued nature of the output field for a given input field (S-shaped OB curve); however, a given output field uniquely determines the input field. A generalization of this strategy fails because it is impossible to choose the amplitude and phase of both the output fields, as the input fields, the cavity fields, and their interaction with the medium self-consistently determine the eventual amplitude and phase of the output fields. Without retaining the identity of the individual fields ( $x_1$  distinct from  $x_2$ ) within the two cavities, one would not obtain the hump-like

feature (discussed below) in the lower branch [24], which is crucial and eventually transforms into negative hysteresis as shown in Fig. 2(a). To deal with such numerical constraints we used, in general, the Newton-Raphson method to obtain the steady-state solution of the nonlinear atom-field equations along with the boundary conditions. In the general dispersive case an *arbitrary* choice of relative strength and phases of the output field does not necessarily correspond to a physically viable input-field variation. The on-resonance case involves real fields, and as indicated earlier, the solution can be obtained in the steady state and acts as a check for the solutions obtained using the Newton-Raphson method.

To mimic a typical experimental situation we use real values for the input fields and compute the resultant complex output fields self-consistently along the different branches of the S-shaped OB response. We also note that, to focus our attention on the low-input-light OB regime, we have avoided regimes involving multistability, which is easily obtained in this double-cavity OB system. We highlight two important features here; the first is the enhancement of the output field at  $\omega_2$  coupling the  $|2\rangle \leftrightarrow |3\rangle$  transition. This arises due to the creation of inversion in the  $|1\rangle \leftrightarrow |2\rangle$  transition and leads to the hump-like response that transforms into the negative-hysteresis loop. The second is the novel switching characteristics wherein the output fields exhibit self-pulsing. The two fields mimic each other in their temporal response. The hump-like feature in the OB response indicates an enhancement of the field at  $\omega_2$  arising due to suppressed absorption along the  $|2\rangle \leftrightarrow |3\rangle$  transition. This occurs in the lower cooperative branch at low intensities of the  $\omega_2$  input field, where initially the population is dominantly in the ground state  $|3\rangle$ . A large cooperative parameter  $C_1$  along the upper transition  $|1\rangle \leftrightarrow |2\rangle$  leads to enhanced interaction with the  $\omega_1$  field resulting in the extraction of a significant fraction of the population into the excited states. Furthermore, as the upper state ( $|1\rangle$ ) population builds up, this results in a lowering of the influence of  $\omega_2$  field on these atoms. This leads to the creation of population inversion between  $|1\rangle$  and  $|2\rangle$ , that is,  $\rho_{11} > \rho_{22}$  [25]. This dynamics occurs due to the asymmetric choice of the cooperative parameters  $C_1 > C_2$  at the cavity resonant condition  $\theta_1 = \theta_2 = 0$ . However, similar dynamics can be obtained for comparable values of  $C_1$  and  $C_2$  in the bad-cavity limit, that is, with finite cavity detuning  $\theta_2$  [22]. An enhancement of the  $\omega_2$  field can be associated with a decrease in absorption  $[\text{Im}\{\rho_{23}\}]$  accompanied by enhanced absorption  $[\text{Im}\{\rho_{12}\}]$  of the  $\omega_1$  field, *with* and *without* the feedback for the  $\omega_1$  field; this clearly demonstrates the reliance of the enhancement on the cavity-assisted inversion [see Figs. 2(b)–2(d)]. With increasing incident field strength  $y_1$ , the above effects are enhanced and the hump-like feature becomes quite exaggerated, eventually resulting in a negative-hysteresis loop as indicated in Fig. 2(a). A similar scenario is observed with increasing cooperative parameter  $C_1$ .

We describe in detail the negative-hysteresis loop arising in this system (Fig. 3). As discussed above the field at  $\omega_2$  is enhanced, however, upon further increase in the input field  $y_2$ , the population from the upper states is drawn back into the lower levels  $|2\rangle$  and  $|3\rangle$ , ultimately leading to large absorption of the  $\omega_2$  field, and the output switches to the *off* state [indicated by  $N_1$  in Fig. 3(a)]. In the reverse direction,

as the input intensity  $y_2$  is decreased the output field switches from the off state to the on state along  $N_2$  (different from  $N_1$ ), thus encompassing within it a negative-hysteresis loop. This hysteresis is exactly opposite to the conventional bistability (we denote as the positive hysteresis), wherein low input intensities lead to a low output intensity, and only for higher input intensities is the transition saturated (for zero atomic detuning), leading to a large output field and the corresponding reverse loop, which encloses a positive hysteresis [labeled  $P_1$  and  $P_2$  in Fig. 3(a)]. Positive hysteresis occurs at higher input field intensities, distinct from the low-input intensity negative-hysteresis region.

The nature of threshold points associated with the negative hysteresis are similar to the positive hysteresis of conventional OB and displays critical slowing-down. The study of the time-dependent switching indicates that, choosing an operating point  $|y_2|_{\text{op}}$  closer to the threshold of switching results in an increase in the time required to switch to the steady state [Figs. 3(b) and 3(c)]. Note that this behavior occurs at all four threshold points  $|y_2|_{\text{th}}$  associated with the switching transitions  $N_{1,2}$  and  $P_{1,2}$ . Variation of any other parameter results in shifting of the threshold point itself and, thus, the associated change in the switching times due to critical slowing-down.

Apart from such multicolored stable switching, the system also exhibits a wealth of dynamics like periodic self-pulsing, wherein a constant input intensity results in periodic output at both frequencies. The periodicity can be controlled using cavity parameters such as  $\kappa_{1,2}$  and  $\theta_{1,2}$  [22]. We would like to point out that the nonlinear dynamics can be obtained in a

robust manner for a wide variety of operational regimes. Before we conclude we indicate that the regime of experimental implementation, for example, in rubidium atomic vapor (along the ladder transition  $5S_{1/2} \leftrightarrow 5P_{3/2} \leftrightarrow 5D_{5/2}$ ), would involve a number density of  $\approx 10^{11}$  atoms/cm<sup>3</sup>, with a transmission coefficient  $T \approx 10^{-1}$ – $10^{-3}$  giving rise to  $C \approx 1000$ , and with an input power varying from  $\approx 0$  to 20 mW across a spot size of 100  $\mu\text{m}$ . The cooperative parameter can be varied by changing either the number density of atoms or the transmission coefficient of the cavity.

#### IV. CONCLUSIONS

In conclusion, we have demonstrated a simple all-optical double-cavity bistable system that exhibits negative as well as positive hysteresis. We self-consistently determine the amplitude and phases of the two output fields. A region of response involving a hump-like feature in the S-shaped OB curves transforms into a negative-hysteresis loop. These effects are a consequence of the cavity-induced inversion arising from the simultaneous cooperative coupling and their interplay at the two frequencies  $\omega_1$  and  $\omega_2$ . The system also exhibits a range of nonlinear dynamical features such as self-pulsing and chaos.

#### ACKNOWLEDGMENTS

One of us (H.A.B.) would like to thank the Indian Institute of Technology Kanpur for financial support. The authors would also like to thank one of the referees for useful insights.

- 
- [1] A. Szoke, V. Daneu, J. Goldhar, and N. A. Kurnit, *Appl. Phys. Lett.* **15**, 376 (1969); H. M. Gibbs, S. L. McCall, and T. N. C. Venkatesan, *Phys. Rev. Lett.* **36**, 1135 (1976); A. Joshi and M. Xiao, *J. Mod. Opt.* **57**, 1196 (2010).
- [2] L. A. Lugiato, *Progress in Optics*, edited by E. Wolf (North-Holland, Amsterdam, 1984), Vol. XXI, p. 69.
- [3] H. M. Gibbs, *Optical Bistability: Controlling Light with Light* (Academic Press, New York, 1985).
- [4] R. Bonifacio and L. A. Lugiato, *Phys. Rev. A* **18**, 1129 (1978); M. Vengalattore, M. Hafezi, M. D. Lukin, and M. Prentiss, *Phys. Rev. Lett.* **101**, 063901 (2008).
- [5] H. M. Gibbs, F. A. Hopf, D. L. Kaplan, and R. L. Shoemaker, *Phys. Rev. Lett.* **46**, 474 (1981); K. Ikeda, H. Daido, and O. Akimoto, *ibid.* **45**, 709 (1980); H. Nakatsuka, S. Asaka, H. Itoh, K. Ikeda, and M. Matsuoka, *ibid.* **50**, 109 (1983); M. Taki, *Phys. Rev. E* **56**, 6033 (1997).
- [6] D. Jaksch, C. Bruder, J. I. Cirac, and C. W. Gardiner, and P. Zoller, *Phys. Rev. Lett.* **81**, 3108 (1998).
- [7] R. Folman, P. Kruger, D. Cassettari, B. Hessmo, T. Maier, and J. Schmiedmayer, *Phys. Rev. Lett.* **84**, 4749 (2000).
- [8] J. D. Pritchard, D. Maxwell, A. Gauguier, K. J. Weatherill, M. P. A. Jones, and C. S. Adams, e-print [arXiv:1006.4087v1](https://arxiv.org/abs/1006.4087v1) [quant-ph].
- [9] H. Schempp, G. Gunter, C. S. Hofmann, C. Giese, S. D. Saliba, B. D. DePaola, T. Amthor, M. Weidemuller, S. Sevincli, and T. Pohl, *Phys. Rev. Lett.* **104**, 173602 (2010).
- [10] R. Heidemann, U. Raitzsch, V. Bendkowsky, B. Butscher, R. Low, L. Santos, and T. Pfau, *Phys. Rev. Lett.* **99**, 163601 (2007).
- [11] W. Harshawardhan and G. S. Agarwal, *Phys. Rev. A* **53**, 1812 (1996).
- [12] A. Joshi and M. Xiao, *Progress in Optics*, edited by E. Wolf (North-Holland, Amsterdam, 2006), Vol. 49, p. 97.
- [13] A. Joshi, A. Brown, H. Wang, and M. Xiao, *Phys. Rev. A* **67**, 041801 (2003).
- [14] W. Yang, A. Joshi, and M. Xiao, *Phys. Rev. Lett.* **95**, 093902 (2005).
- [15] The two-photon Doppler broadening is canceled to first order by choosing a counter-propagating beam in the ladder system, because atoms with velocity  $v$  have the polarization  $\rho_{13} \propto [\gamma_1 + (\Delta_1 + k_1 v) + (\Delta_2 - k_2 v)]^{-1}$ .
- [16] A. Joshi, W. Yang, and M. Xiao, *Phys. Rev. A* **70**, 041802 (2004).
- [17] B. Segard, B. Macke, L. A. Lugiato, F. Prati, and M. Brambilla, *Phys. Rev. A* **39**, 703 (1989).
- [18] L. M. Narducci, W. W. Eidson, P. Furcinitti, and D. C. Eteson, *Phys. Rev. A* **16**, 1665 (1977); P. Galatola, L. A. Lugiato, M. Vadamchino, and N. B. Abraham, *Optics Commun.* **69**, 414 (1989).
- [19] G. P. Agrawal and C. Flytzanis, *Phys. Rev. Lett.* **44**, 1058 (1980).

- [20] L. A. Lugiato, L. M. Narducci, D. K. Bandy, C. A. Pennise, *Optics Commun.* **43**, 281 (1982).
- [21] P. Grangier, J. F. Roch, J. Roger, L. A. Lugiato, E. M. Pessina, G. Scandroglio, and P. Galatola, *Phys. Rev. A* **46**, 2735 (1992).
- [22] H. A. Babu and H. Wanare, following paper, *Phys. Rev. A* **83**, 033819 (2011).
- [23] R. Bonafacio and L. A. Lugiato, *Optics Commun.* **19**, 172 (1976).
- [24] A. Joshi and M. Xiao, *Appl. Phys. B* **79**, 65 (2004).
- [25] In another context, steady-state inversion arising due to quantum fluctuations has been proposed by C. M Savage, *Phys. Rev. Lett.* **60**, 1828 (1988).